Critical behavior of the spin-$\frac{3}{2}$ Blume-Capel model in two dimensions

J. C. Xavier and F. C. Alcaraz
Departamento de Física, Universidade Federal de São Carlos, 13565-905, São Carlos, SP, Brazil

D. Penã Lara* and J. A. Plascak
Departamento de Física, Universidade Federal de Minas Gerais, 30161-970, Belo Horizonte, MG, Brazil

(Received 25 November 1997)

The phase diagram of the spin-$\frac{3}{2}$ Blume-Capel model in two dimensions is explored by conventional finite-size scaling, conformal invariance, and Monte Carlo simulations. The model in its τ-continuum Hamiltonian version is also considered and compared with other spin-$\frac{3}{2}$ quantum chains. Our results indicate that, different from the standard spin-1 Blume-Capel model, there is no multicritical point along the order-disorder transition line. This is in qualitative agreement with mean-field prediction, but in disagreement with previous approximate renormalization-group calculations. [S0163-1829(98)06417-0]

I. INTRODUCTION

The Spin-S Blume-Capel Model is a generalization of the standard Ising model with dynamics described by the Hamiltonian

$$H=-J\sum_{\langle i,j\rangle} s_i s_j + D\sum_i s_i^2, \tag{1}$$

where the first sum runs over all nearest neighbors and the spin variables s_i assume values $-S,-S+1,\ldots,S$, associated with each site i of the lattice. In Eq. (1) J is the exchange coupling and D is a single spin anisotropy parameter. In the case where $S=1$ this Hamiltonian was proposed originally by Blume and Capel[1] for treating magnetic systems and has also been used in describing ^{3}He-^{4}He mixtures.[2] This $S=1$ model was studied by a variety of methods such as mean field,[1] two-spin cluster,[3] variational methods,[4] constant coupling approximation,[5] Monte Carlo simulations,[6,7] finite-size scaling on its transfer matrix[8] or quantum Hamiltonian[9,10] and renormalization-group methods.[11,12] It is well established that for dimension $d\geqslant 2$ the $S=1$ model presents a phase diagram with ordered ferromagnetic and disordered paramagnetic phases separated by a transition line that changes from a second-order character (Ising type) to a first-order one at a tricritical point. More specifically, in two dimensions the machinery coming from conformal invariance[13,14] indicates that at this tricritical point the long-range fluctuations are governed by a conformal field theory with central charge $c=\frac{7}{10}$ (Refs. 9 and 10). In this case all the critical exponents and the whole operator content of the model are obtained.[10]

For values of spin $S>1$ however the situation is quite unclear, with fewer results and contradictions among them. The mean-field calculation[15] (see also Ref. 16) predicts different phase diagrams for integer or half-odd-integer spins. For spin $S=\frac{3}{2}$ it gives a second-order phase transition with no tricritical point and a separated first-order transition line that ends up in an isolated multicritical point. In contradiction with these results a calculation[12] based on a renormalization group introduced in Ref. 17 gives us, for the two-dimensional model, a unique first-order transition line at low temperature that ends up in the second-order transition line at a tetracritical point. Similar results are also obtained by using a Migdal-Kadanoff real-space renormalization-group approach.[18]

Motivated by these contradictions, we decided to study extensively the two-dimensional $S=\frac{3}{2}$ model by using conformal invariance and finite-size scaling, since these methods give us, in the $S=1$ model, the most precise and conclusive results. In order to supplement our conclusions, in the $S=\frac{3}{2}$ model, we also perform Monte Carlo simulations in the region of the phase diagram where multicritical behavior might occur.

The layout of this paper is as follows. In Sec. II the transfer matrix of the model and the relations used in our finite-size studies are presented. In Sec. III we discuss initially our results for the $S=1$ model. Although the phase diagram is well established, we believe that our numerical estimate for the tricritical point is the most precise in the present literature. In Sec. IV our results for the spin-$\frac{3}{2}$ is presented and discussed. In Sec. V we study the spin-$\frac{3}{2}$ model in its τ-continuum formulation and compare its quantum Hamiltonian with another spin-$\frac{3}{2}$ quantum chain that is known to present a multicritical point along the order-disorder phase transition line. In Sec. VI we close our paper with a summary and conclusions of our main results. Finally, in Appendix A the details and methods of our Monte Carlo simulations for the spin-$\frac{3}{2}$ model are explained.

II. TRANSFER MATRIX AND CONFORMAL INVARIANCE RELATIONS

The row-to-row transfer matrix $\hat{T}$ of the Hamiltonian (1) in a square lattice, with horizontal width N has dimension $(2S+1)^N\times(2S+1)^N$. Its coefficients $\langle s_1',\ldots,s_N'|\hat{T}|s_1,\ldots,s_N\rangle$ are the Boltzmann weights generated by the spin configurations $\{s_1,\ldots,s_N\}$ and $\{s_1',\ldots,s_N'\}$ of adjacent rows. In general, if we consider Eq. (1) with periodic or free boundary conditions in the horizontal direction, the matrix $\hat{T}$ will have all its elements nonzero,

being a dense matrix. This difficulty restricts the numerical study for very small lattices. A possible way to reach larger lattices, with reasonable computational effort, is to consider the model in its τ-continuum limit.[19] In this case, after a high anisotropic limit of its couplings in the vertical and horizontal directions, we replace the transfer matrix by a simpler effective quantum Hamiltonian that is a sparse matrix. Most of the finite-size scaling studies exploring conformal invariance for general models were done in this formulation. However, in such an approach the calculation of the transition lines, in terms of the original coupling (isotropic), is not possible. Another possibility, which is suitable for our purposes, is to impose helical boundary conditions along the horizontal direction. In this case the transfer matrix can be written as

$$\hat{T}=\hat{t}^N, \tag{2}$$

where $\hat{t}$ is the transfer submatrix with elements given by

$$\langle s_1,\ldots,s_N|\hat{t}|s_1',\ldots,s_N'\rangle = \exp[t^{-1}s_1(s_2+s_N')-dt^{-1}s_1^2]\prod_{j=1}^{N-1}\delta_{s_{j+1},s_j'}, \tag{3}$$

with $t=k_BT/J$ (k_B is the Boltzmann constant) and $d=D/J$. We also see from Eqs. (2) and (3) that although $\hat{T}$ is a dense matrix, $\hat{t}$ is a sparse one, having only a fraction $f=\exp[-(N-1)\ln(2S+1)]$ of nonzero elements. The Hamiltonian (1), like the standard Ising model, has a global $Z(2)$ symmetry. The helical boundary condition does not break this symmetry, which translates in the commutation of $\hat{t}$ with the parity operator

$$\hat{P}=\prod_{i=1}^{N}\hat{R}_l,$$

where $\hat{R}_l=1\otimes1\otimes\cdots1\otimes\hat{R}\otimes1\cdots\otimes1$, and $\hat{R}$, located at lth position in the product, are $(2S+1)\times(2S+1)$ matrices given by

$$\hat{R}=\sum_{s=-S}^{S}|s\rangle\langle -s|.$$

Consequently, in the basis where $\hat{P}$ is diagonal, we can separate the vector space associated to $\hat{T}$ into two disjoint sectors labeled by the eigenvalues $p=\pm1$ of the parity operator.

Let us for convenience introduce the Hamiltonian matrix $\hat{H}=-\ln(\hat{T})=-N\ln(\hat{t})$, and denote by the $e_{l,p}$ the lth lowest ($l=1,2,\ldots$) eigenvalue in the sector with parity p. The eigenenergies of the ground state and first excited state are given by $e_{1,1}$ and $e_{1,-1}$, respectively. These two leading energies, and consequently the mass gap $G_N(t,d)=e_{1,-1}-e_{1,1}$, for a system of width N are real and can be obtained for relative large N by a direct application of the power method.[20] The standard finite-size scaling[21] gives an estimate of the phase transition curve $t_c=t_c(d)$. This curve is evaluated by extrapolations to the bulk limit ($N\to\infty$) of sequences $t_c(d,N)$ obtained by solving

$$G_N(t_c)N=G_{N+1}(t_c)(N+1)\quad N=2,3,\ldots. \tag{4}$$

An heuristic method, which was proved to be effective in obtaining multicritical points in earlier works[9,22,23] is to simultaneously solve Eq. (4) for three different lattice sizes,

$$G_N(t_c)N=G_{N+1}(t_c)(N+1)=G_{N+2}(t_c)(N+2)\qquad N=2,3,\ldots. \tag{5}$$

Once the transition curve is estimated, in the region of continuous phase transition we expect the model to be conformal invariant. This symmetry allows us to infer the critical properties from the finite-size corrections of the eigenspectrum at t_c.[13,14] The appropriate relations that give the scaling dimensions and conformal anomaly in the case of periodic or free boundary conditions are well known in the literature.[13,14] In the present case, where we impose helical boundary conditions, these relations are slightly different from the periodic case since translational invariance is lost in the horizontal direction. The conformal anomaly c, which labels the universality class, can be calculated from the large-N behavior of the ground-state energy

$$\frac{e_{1,1}(N)}{N}=\epsilon_\infty-\frac{\pi c v_s}{6N^2}+o(N^{-2}), \tag{6}$$

where ϵ_∞ is the ground-state energy per site, in the bulk limit, and v_s, which is unity in our transfer matrix calculations, is the sound velocity. The scaling dimensions of operators governing the critical fluctuations (related to critical exponents) are evaluated from the finite-N corrections of the excited states. For each primary operator, with dimension x_ϕ, in the operator algebra of the system, there exists an infinite tower of eigenstates of $\hat{H}$ whose energy $e^{\phi}_{m,m'}$ are given by

$$\mathrm{Re}[e^{\phi}_{m,m'}(N)]=e_{1,1}+\frac{2\pi v_s}{N}(x_\phi+m+m')+o(N^{-1}), \tag{7}$$

where $m,m'=0,1,\ldots$. The real part of the energies appears in Eq. (7) since in general they are complex due to the nonhermicity of $\hat{H}$. The multiplicity of energies with the same real part $\mathrm{Re}[e^{\phi}_{m,m'}(N)]$ are given in terms of the product of two Virasoro algebras, as in the periodic case. We tested extensively the relations (6) and (7) for several excited eigenenergies in the case of the Ising model with helical boundary conditions.

III. THE SPIN-1 MODEL

In order to test our numerical methods and the conformal invariant relations (6) and (7), we consider initially the Blume-Capel model with spin $S=1$. Earlier finite-size studies that explored the conformal invariance of this model were done in its τ-continuum formulation.[9,10] In Fig. 1 we show the extrapolated ($N\to\infty$) transition curve $t_c=t_c(d)$ (continuum line in the figure) obtained by solving Eq. (4) for lattice sizes up to $N=12$. Note that for $d\ll-1$ only configurations where $s_i=\pm1$ are allowed, and we have an effective Ising model with $t_c=2/\ln(\sqrt{2}+1)=2.269\ldots$.

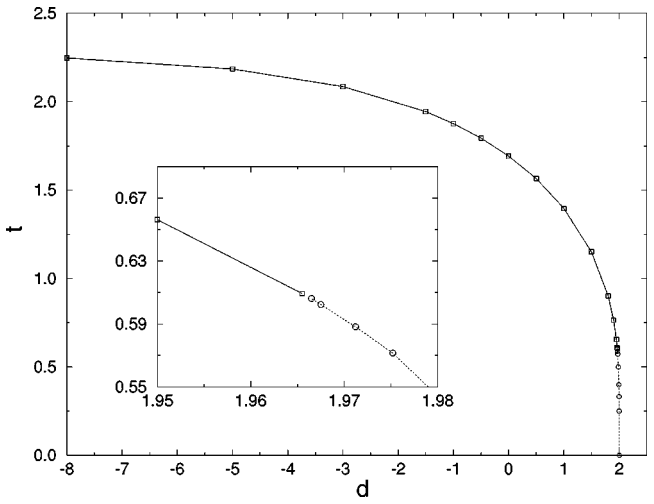

FIG. 1. Phase diagram in the (d-t) plane for the spin-1 Blume-Capel model. The continuum line is the second-order transition line and the dotted line is the first-order transition. The tricritical point is located at the end point of the continuum line.

The expected tricritical point of the model is obtained by extrapolating the sequences obtained by solving Eq. (5). Our estimate for this point is $t_t=0.609(4)$ and $d_t=1.965(5)$ [we solved Eq. (5) for lattice sizes up to $N=10$], in agreement with previous Monte Carlo[7] and finite-size calculations.[8] In Ref. 8 these estimates were done from data of lattice sizes up to $N=8$. The extrapolations along this paper were obtained by using the ϵ-alternated van den Broeck–Schwartz (VBS) approximation.[24] The errors are estimated from the stability of the extrapolations and are in the last digit. In Fig. 1 we show in a large scale the region where the tricritical point is located. In this figure this point is the end point of the continuum curve.

Strictly speaking, the relation (4) only gives continuous phase transitions. At the first-order line, in the spin-1 model, we have the coexistence of three phases: two ordered ferromagnetic ($\langle s_i\rangle\neq 0$) and one disordered phase ($\langle s_i\rangle=0$). Consequently, the gaps related with the three lowest eigenvalues vanishes exponentially as the lattice size increases. A possible finite-size estimate for the first-order transition line, which we test in this paper, is obtained by the following procedure. For a given lattice size N we calculate the points where the gap corresponding to the third eigenvalue has its minimum value. The extrapolation $N\to\infty$ of these points give us our estimate for the first-order transition line. The dotted line shown in Fig. 1 was obtained by this procedure. As we can see in this figure, the estimated first-order transition line (dotted line) finishes at the tricritical point.

In the critical regions of the phase transition line (continuum curve) the conformal anomaly and the scaling dimensions can be calculated exploring the conformal invariant relations (6) and (7). From Eq. (6) a possible way to extract c is by extrapolating the sequence

$$c^{N,N+1}=\frac{6}{\pi}\left(\frac{e_{1,1}(N+1)}{N+1}-\frac{e_{1,1}(N)}{N}\right)\left(\frac{1}{N^2}-\frac{1}{(N+1)^2}\right)^{-1}, \tag{8}$$

calculated at $t_c(d)$. Examples of such sequences together with the extrapolated results for the spin-1 model, are shown in the first four columns of Table I. We clearly see from this table the expected results, i.e., an Ising behavior with conformal anomaly $c=\frac{1}{2}$ in the left of tricritical point (continuum curve) and $c=\frac{7}{10}$ at the tricritical point.

From Eq. (7) the scaling dimensions $x(n,p)$ related to the nth ($n=1,2,\ldots$) energy in the sector with parity p can be obtained by extrapolating the sequence

$$x^N(n,p)=\frac{\{\mathrm{Re}[e_{n,p}^{(N)}]-e_{1,1}(N)\}N}{2\pi}. \tag{9}$$

The smallest dimension $x(1,-1)$ corresponds to a $Z(2)$ order parameter. Some of the related finite-size sequences are presented in the first four columns of Table II for the spin-1 model. As expected, this dimension has the value $\frac{1}{8}$ for the critical points in the Ising universality class and $3/40=0.075$ at the tricritical point. The conformal towers at the tricritical point were obtained previously by using the τ-continuum Hamiltonian formulation of the model.[9,10]

TABLE I. Finite-size data $c^{N,N+1}$ given by Eq. (8) and extrapolations for the conformal anomaly for some values of d. The first four columns are the values for the $S=1$ model while the last four are those of the $S=\frac{3}{2}$ model.

	$S=1$				$S=\frac{3}{2}$			
N	$d=-0.5$ $t_c=1.794(7)$	$d=0$ $t_c=1.681(5)$	$d=1.9$ $t_c=0.764(7)$	$d=1.9655$ $t_c=0.609(4)$	$d=-0.5$ $t_c=3.549(8)$	$d=0$ $t_c=3.287(2)$	$d=0.5$ $t_c=2.972(3)$	$d=2$ $t_c=0.64(7)$
4	0.460 931	0.461 723	0.570 695	0.641 586	0.461 970	0.463 160	0.465 282	0.626 807
5	0.478 008	0.478 429	0.578 328	0.666 641	0.478 574	0.479 283	0.480 650	0.611 765
6	0.486 062	0.486 307	0.575 809	0.678 638	0.486 400	0.486 858	0.487 798	0.589 182
7	0.490 323	0.490 480	0.569 959	0.685 059	0.490 544	0.490 864	0.491 549	0.568 249
8	0.492 838	0.492 948	0.563 332	0.688 878	0.492 994	0.493 232	0.493 754	0.551 328
9	0.494 458	0.494 539	0.556 880	0.691 349	0.494 573	0.494 758	0.495 170	0.538 405
10	0.495 569	0.495 633	0.550 943	0.693 048	0.495 659	0.495 807	0.496 142	0.528 798
11	0.496 370	0.496 421	0.545 616	0.694 269	0.496 440	0.496 562	0.496 841	0.521 749
12	0.496 968	0.497 009	0.540 896	0.695 175				
13	0.497 427	0.497 462	0.536 738	0.695 864				
14	0.497 788	0.497 817	0.533 085	0.696 401				
∞	0.499(9)	0.499(9)	0.50(3)	0.698(9)	0.499(8)	0.499(8)	0.499(8)	0.50(5)

TABLE II. Finite-size data $x^N(1,-1)$ given by Eq. (9) and extrapolations for the scaling dimension of the parameter order for some values of d. The first four columns are the values for the $S=1$ model while the last four are those of the $S=3/2$ model.

	$S=1$				$S=\frac{3}{2}$			
$N\backslash d$	-0.5	0	1.9	1.9655	-0.5	0	0.5	2
4	0.118 424	0.118 238	0.100 130	0.071 623	0.118 424	0.117 745	0.117 610	0.089 071
5	0.121 069	0.120 923	0.105 237	0.073 095	0.121 185	0.120 449	0.120 484	0.100 904
6	0.122 389	0.122 278	0.108 791	0.073 783	0.122 612	0.121 806	0.121 985	0.108 882
7	0.123 137	0.123 049	0.111 422	0.074 134	0.123 454	0.122 565	0.122 863	0.113 933
8	0.123 602	0.123 532	0.113 439	0.074 315	0.124 003	0.123 022	0.123 424	0.117 077
9	0.123 913	0.123 855	0.115 022	0.074 400	0.124 391	0.123 312	0.123 807	0.119 047
10	0.124 132	0.124 082	0.116 285	0.074 425	0.124 683	0.123 500	0.124 082	0.120 304
11	0.124 292	0.124 248	0.117 305	0.074 409	0.124 913	0.123 625	0.124 287	0.121 121
12	0.124 413	0.124 373	0.118 136	0.074 362	0.125 102	0.123 706	0.124 446	0.121 662
13	0.124 507	0.124 470	0.118 821	0.074 290				
14	0.124 582	0.124 547	0.119 387	0.074 199				
15	0.124 642	0.124 608	0.119 860	0.074 091				
∞	0.1250(0)	0.1250(2)	0.12(2)	0.074(0)	0.13(0)	0.123(8)	0.125(5)	0.122(2)

In order to compare our estimate for the tricritical point with the previous results we have also calculated the conformal anomaly and scaling dimensions by using the tricritical point estimated in Refs. 7 and 8. These results show us that the extrapolated values of the conformal anomaly is similar to ours, however our estimate for the scaling dimensions are much better than the values obtained at their estimated tricritical point. For these reasons we believe that the tricritical point we found is a better estimate.

IV. THE SPIN-$\frac{3}{2}$ MODEL

We now apply the numerical methods of Sec. II in the controversial case of spin $\frac{3}{2}$. In Fig. 2 we show the extrapolated transition curve $t_c=t_c(d)$ (continuum line), obtained by solving Eq. (4) for lattice sizes up to $N=10$. The limiting values $t_c=9/[2\ln(\sqrt{2}+1)]=5.106\ldots$ $(d\ll -1)$ and $t_c=1/[2\ln(\sqrt{2}+1)]=0.567\ldots(d\gg 1)$ can be easily understood since in these limits the model reduces to an Ising model.

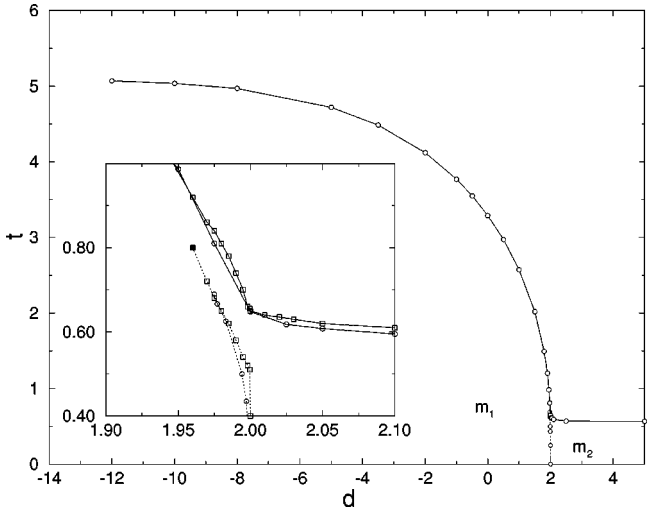

FIG. 2. Phase diagram in the $(d$-$t)$ plane for the spin-$\frac{3}{2}$ Blume-Capel model. The continuum line is the second-order transition line and the dotted line is the first-order transition. The circles were obtained by finite-size estimates and the squares by Monte Carlo. The full square represents the corresponding isolated multiphase critical point. There are two different ferromagnetic phases with $m_1\to\frac{3}{2}$, and $m_2\to\frac{1}{2}$ as $T\to 0$. The open squares in the blown-up region $1.90\leqslant d\leqslant 2.10$ are obtained by Monte Carlo simulations.

As we mentioned in the Introduction, there is a controversy in the literature concerning the existence or not of a multicritical point along the transition line. In order to clarify this point we try to obtain finite-size estimates for this point by using relation (5). Our results however show no consistent solutions of relations (5) for lattice sizes up to $N=10$, which indicate the absence of a multicritical point along the transition line. Another method, also used to locate multicritical points,[22] is obtained from the simultaneous crossing of two different gaps on a given pair of lattices [instead of three lattices as in Eq. (4)]. Trying several different gaps we also did not find, within this method, a multicritical point along the transition curve.

The first-order transition line was also estimated in a similar way as we did for the spin-1 model in the last section. Along this line we have the coexistence of four ordered phases, with most of spins in state $s=\pm\frac{3}{2}$, $\frac{1}{2}$ or $-\frac{1}{2}$, respectively. The finite-size estimator, for a given N, is given by the points where the fourth gap has its minimum value, since in the bulk limit the four lowest eigenenergies will degenerate. The extrapolated curve $(N\to\infty)$ is the dotted curve shown in Fig. 2. As depicted in a large scale in this figure, this first-order transition line does not touch the continuous transition line (differently from the case $S=1$), in agreement with the topology predicted for the phase diagram by mean-field calculations.[15]

In order to supplement our results by an independent method we also did Monte Carlo simulations for the spin-$\frac{3}{2}$ model. Details of the simulations are presented in Appendix A. The points for the phase diagram are the squares shown in Fig. 2. Taking into account the scale of this figure, the agreement of the Monte Carlo simulations (squares) and the transfer-matrix results (circle) is good. These results indicate

the absence of a multicritical point along the continuous transition line. According to this scenario the whole continuous phase-transition line should belong to the Ising universality class. In order to illustrate this point, we present in the last four columns of Table I, for some values of d, the finite-size sequences (8) of the conformal anomaly of the model. In the last four columns of Table II we also show some of finite-size sequences (9) for the dimension $x(1,-1)$ of the order parameter. Again, we obtain the expected results $\frac{1}{8}$ of the Ising-order parameter.

As usual, in the region where the first-order phase transition takes place, the finite-size sequences have slower convergence due to crossover effects. This fact prevents us from obtaining a good estimate for the endpoint of the first-order transition line. Our Monte Carlo simulations (see appendix A) give an estimate, $t_I=0.80$ and $d_I=1.96$, for this point.

V. THE τ-CONTINUUM QUANTUM HAMILTONIAN OF THE SPIN-$\frac{3}{2}$ MODEL AND OTHER RELATED QUANTUM CHAINS

Our results in the last section indicate that the spin-$\frac{3}{2}$ Blume-Capel model does not have a multicritical point along the transition line that separates the disordered phase from the ordered ones. Instead of working in the Euclidean version, we can also consider the model in its τ-continuum Hamiltonian formulation. This quantum Hamiltonian, which is obtained by imposing extreme anisotropic relations between its couplings in the horizontal and vertical directions, can be derived straightforwardly (see Ref. 19, for example). For periodic boundary conditions it is given by $\hat{H}(b=1)$ where

$$\hat{H}(b)=-\sum_{i}^{N}\hat{S}_i^z\hat{S}_{i+1}^z-x_1(\hat{S}_i^z)^2-x_2\hat{R}_i(b), \qquad (10)$$

and x_1 and x_2 are coupling constants. The operators $\hat{S}_i$ and $\hat{R}_i(b)$ in the basis where $\hat{S}_i$ is diagonal are given by

$$\hat{S}_i^z=1\otimes 1\otimes\cdots 1\otimes S^z\otimes 1\cdots\otimes 1,$$

$$\hat{R}_i(b)=1\otimes 1\otimes\cdots 1\otimes R(b)\otimes 1\cdots\otimes 1,$$

where the matrices S^z and $R(b)$ are in the ith position in the product and are given by

$$R=\begin{pmatrix}0&1&0&0\\1&0&b&0\\0&b&0&1\\0&0&1&0\end{pmatrix}\quad S^z=\begin{pmatrix}\frac{3}{2}&0&0&0\\0&\frac{1}{2}&0&0\\0&0&-\frac{1}{2}&0\\0&0&0&-\frac{3}{2}\end{pmatrix}. \qquad (11)$$

Diagonalizing the Hamiltonian (10) for several lattices we try to locate a multicritical point, by solving Eq. (4). In agreement with the absence of multicritical behavior, we found no triple crossing for lattice sizes $N>4$.

It is important to mention that, contrary to these results, the spin-$\frac{3}{2}$ Hamiltonian $\hat{H}(2/\sqrt{3})$, given by Eq. (10), is known to have a tetracritical point along the transition line separating the disordered and ordered line.[23,25] The matrices S^z and $R(2/\sqrt{3})$, given in (11), are in this case the standard S_z-diagonal representation of the spin-$\frac{3}{2}$ SU(2) matrices. This tetracritical point was located[23] by the same techniques we used in this paper and its long-distance physics is related by a conformal field theory with central charge $c=\frac{4}{5}$. It is interesting to observe that such a small difference in the Hamiltonians produce such differences in the critical behavior of the Hamiltonians. In order to better see this fact numerically, we study the Hamiltonian (10) with b ranging from 1 to $2/\sqrt{3}$. We verify that the solutions of Eq. (7) for multicritical points happens only for values of b bigger than, or very close to, $2/\sqrt{3}$.

These results in the quantum Hamiltonian formulation indicate that multicritical points along the order-disorder line can be generated only if we introduce additional interactions in the spin-$\frac{3}{2}$ Blume-Capel model. The net effect of the coupling b in the quantum chain (10) is to control the preference for neighboring spins (s,s') along the time (vertical) direction to be in pairs $(\frac{1}{2},-\frac{1}{2})$ or $(-\frac{1}{2},\frac{1}{2})$. One possible way to introduce this effect in the classical model is to add in the spin-$\frac{3}{2}$ Blume-Capel (1) Hamiltonian an extra term $V_{s,s'}(\alpha)=-\alpha(\delta_{s,1/2}\delta_{s',-1/2}+\delta_{s',1/2}\delta_{s,-1/2})$, along all the links in the vertical. The product $\beta\alpha$ will play a similar role as b in Eq. (10). Studying numerically the transfer matrix of such classical Hamiltonian we found for $\alpha=1$ a multicritical point at $t_t=0.87(8)$ and $d_t=1.60(5)$. Our calculations at this point are in favor of a value $c=\frac{4}{5}$ and $x(1,-1)=0.05$ for the conformal anomaly and the dimension of most relevant order parameter, respectively. These are the predicted values for a minimal conformal theory with $m=5$.[25]

VI. SUMMARY AND CONCLUSION

Our aim in this paper was the study of the critical properties of the spin-$\frac{3}{2}$ Blume-Capel model by using the methods of finite-size scaling in strip geometries, conformal invariance, and Monte Carlo simulations. The methods and useful relations for these calculations were presented in Sec. II and in Appendix A, and were tested for the spin-1 Blume-Capel model with a precise evaluation of its phase diagram. Our results for the spin $\frac{3}{2}$ help to choose between the two existing contradictory predictions for its phase diagram in (t,d)-parameter space. Mean-field calculations[15] predict (scenario a) a phase diagram where there is no multicritical point along the second-order phase transition line. In this scenario a multicritical point will exist as an isolated end point of a first-order transition line. On the other hand, approximate calculations based on renormalization-group methods in real space[11,12] give us (scenario b) a multicritical point along the disorder-order transition line. This point being the end point of the first-order transition line. Since the mean-field approximation is expected to be correct only for high dimensions, and the other calculations predicting scenario b were done directly in two dimensions, we would expect, at least for two dimensions, scenario b as the correct one. In parallel to these results there exist in the literature[23,25] precise calculations on a related spin-$\frac{3}{2}$ quantum chain, which also indicate a multicritical point along the transition line. Although these calculations were done in a quantum Hamil-

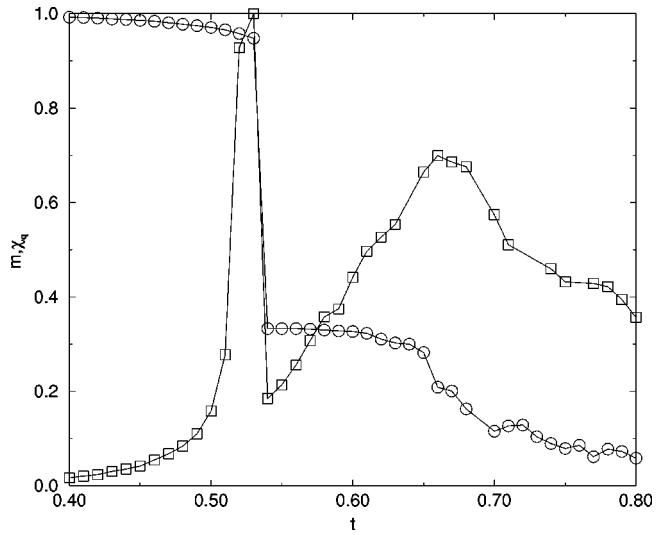

FIG. 3. Quadrupolar susceptibility (open squares) and magnetization (open circles) as a function of t for the Blume-Capel model with $S=\frac{3}{2}$ and $d=1.998$. χ_q has a strong peak only close to $t=0.52$ and the magnetization a discontinuity of about 0.94, indicating a first-order transition. The data were taken for increasing t. The lines are guides to the eyes. The data have been normalized: the maximum magnetization is $m=1.499$ and the maximum susceptibility is $\chi_q=2.02$.

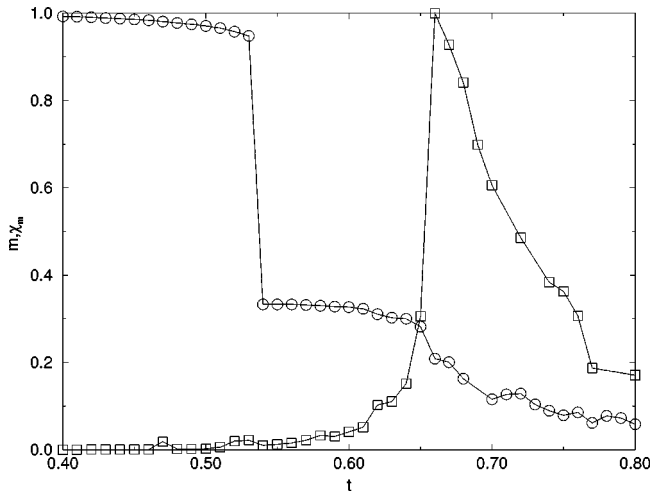

FIG. 4. Magnetic susceptibility (open squares) and magnetization (open circles) as a function of t for the Blume-Capel model with $S=\frac{3}{2}$ and $d=1.998$. χ_m has a strong peak only close to $t=0.66$ and the magnetization is continuous, indicating a second-order transition. The data were taken for increasing t. The lines are guide to the eyes. The data have been normalized: the maximum magnetization is $m=1.499$ and the maximum susceptibility is $\chi_m=53.6$.

tonian, these results incline us to favor scenario b, since this quantum version chain [$\hat{H}(2/\sqrt{3})$ in Eq. (10)] has naively the same type of couplings as the spin-$\frac{3}{2}$ Blume-Capel Model.

However, to our surprise, our results presented in Sec. IV indicate scenario a as the correct one for the spin-$\frac{3}{2}$ Blume-Capel Model. In Sec. V we also analyze this last model in its τ-continuum Hamiltonian formulation [$\hat{H}(1)$ in Eq. (10)] for the sake of comparison with the above mentioned spin-$\frac{3}{2}$ quantum chain [$\hat{H}(2/\sqrt{3})$ in Eq. (10)], which shows multicritical behavior along the order-disorder transition line. Although these Hamiltonians are very similar, our finite-size scaling studies indicate that these differences are enough to produce quite distinct critical behavior. The results of Sec. V also indicate that a phase diagram for a spin-$\frac{3}{2}$ model like that in scenario b can be produced by adding extra terms in the Blume-Capel model.

ACKNOWLEDGMENTS

This work was supported in part by CNPq, CAPES, FAPESP, FAPEMIG, and FINEP-Brazil.

APPENDIX A: MONTE CARLO SIMULATIONS

Our Monte Carlo simulations for the spin-$\frac{3}{2}$ Blume-Capel model were done on square lattices with N^2 sites and periodic boundary conditions in all directions. We have used the standard single spin-flip algorithm[26] where the transition probability P_{ij} from a system configuration with energy E_i (where a chosen spin is in a state i) to another configuration with energy E_j (where this spin is now in a state j) is

$$P_{ij}=\frac{1}{2}\left[1-\tanh\frac{(\beta\Delta E_{ij})}{2}\right],$$

where $\Delta E_{ij}=E_j-E_i$. Since the spin variable can assume more than two states we have chosen, at random, the state j from the $(2S-1)$ possible distinct states from state i.

The thermodynamic quantities computed in these simulations are the magnetization per site

$$m=\langle M\rangle,$$

the magnetic susceptibility

$$\chi_m=\beta N^2\langle(M-m)^2\rangle,$$

where

$$M=\frac{\sum_i s_i}{N^2},$$

and the quadrupole magnetic susceptibility

$$\chi_q=\beta N^2\langle(q-\langle q\rangle)^2\rangle,$$

where

$$q=\frac{\sum_i s_i^2}{N^2}.$$

Typical runnings have been made on a periodic lattice with $N=64$ spins and included 6.0×10^4 iterations or Monte Carlo Steps (MCS) per spin of the algorithm and the averages of the measured quantities were taken after discarding the first 1.0×10^4 MCS per spin. We have found that by changing the lattice size from $N=64$ to $N=128$ the relevant measured quantities did not change appreciably. For this reason, in most of the computations we have taken $N=64$ in order to save computing time. In addition, we have also cal-

culated some Monte Carlo averages taking data from (i) every MCS per spin, (ii) every 10 MCS per spin, and (iii) runnings including 1.2×10^5 MCS per spin with averages taken after discarding the first 2.0×10^4 MCS per spin. In all these runnings, no significant differences have been observed in the thermodynamic quantities of interest when compared to the typical one previously stated in the beginning of this paragraph. These results assure us that possible correlations among different configurations, if any, are not relevant for the computation of the magnetization and susceptibilities. Indeed, our results, within the present numerical precision, are good enough to be compared to other values obtained from different methods. For instance, at $d=0$ we have $t=3.32$ and in the spin-$\frac{1}{2}$ Ising limit $d\rightarrow\infty$, we have $t=0.58$, which is comparable to the exact value $t=0.57$.

The simulations for the phase diagram close to the isolated multiphase critical point are shown in Fig. 2. Second-order phase transitions have been determined by the strong peak in the magnetic susceptibility χ_m, while first-order transitions have been located through the discontinuous behavior of the magnetization accompanied by a strong peak in the quadrupole susceptibility χ_q. A typical example is shown in Figs. 3 and 4 for $d=1.998$ as a function of the reduced temperature t. Such behavior of χ_q is useful for detecting first-order transitions when the discontinuity in the magnetization of the two ordered phases is very small. The discrepancy between the Monte Carlo simulations and finite-size calculations for d very close to 2 reflects the large metastability of the ordered phases. For instance, a metastable phase with $m=\frac{3}{2}$ will persist at low temperatures for d slightly above 2 due to the ordering state starting configuration ($m=\frac{3}{2}$). In fact, by taking a random-state starting configuration and sweeping up and down the temperature for constant $d\geqslant2$, the only stable phase found is the one having $m=\frac{1}{2}$ for $T=0$. The point at $d=2.0$ and $t=0.4$ has not been simulated and is shown in Fig. 2 just for the sake of clarity.

The isolated multiphase critical point in the ordered phase is rather difficult to be located with reasonable precision through Monte Carlo simulations (an estimate can be given by $d_I=1.96$ and $t_I=0.80$). Despite that, we have carefully swept paths of constant temperatures for $t\geqslant0.81$ and constant d for $d\geqslant1.92$ and we have not found any indication of the first-order line, separating the low temperature ordered phases, terminating in the second-order transition line. This is in disagreement with previous renormalization-group calculations[12,18] and reproduce the qualitative behavior predicted by mean-field-like calculations,[15] and are in agreement with our results of finite-size calculations on strips (see Fig. 2).

*Present address: Departamento de Fisica, Universidad del Valle, AA 25360-Cali-Colombia.

[1] M. Blume, Phys. Rev. **141**, 517 (1966); H. W. Capel, Physica (Amsterdam) **32**, 966 (1966).
[2] M. Blume, V. J. Emery, and R. B. Griffiths, Phys. Rev. A **4**, 1071 (1971).
[3] S. L. Lock and B. S. Lee, Phys. Status Solidi B **124**, 593 (1984).
[4] W. Man Ng and J. H. Barry, Phys. Rev. B **17**, 3675 (1978).
[5] M. Tanaka and K. Takahashi, Phys. Status Solidi B **93**, K85 (1979).
[6] A. K. Jain and D. P. Landau, Phys. Rev. B **22**, 445 (1980); O. F. de Alcântara Bonfim and C. H. Obcemea, Z. Phys. B **64**, 469 (1986).
[7] N. B. Wilding and P. Nielaba, Phys. Rev. E **53**, 926 (1996).
[8] P. D. Beale, Phys. Rev. B **33**, 1717 (1986).
[9] F. C. Alcaraz, J. R. D. de Felicio, R. Köberle, and J. F. Stilck, Phys. Rev. B **32**, 7469 (1985).
[10] D. B. Balbão and J. R. Drugowich de Felicio, J. Phys. A **20**, L207 (1987); G. v. Gehlen, *ibid.* **24**, 5371 (1990).
[11] A. N. Berker and M. Wortis, Phys. Rev. B **14**, 4946 (1976); O. F. de Alcântara Bonfim, Physica A **130**, 367 (1985).
[12] S. M. de Oliveira, P. M. C. de Oliveira, and F. C. de Sá Barreto, J. Stat. Phys. **78**, 1619 (1995).
[13] J. L. Cardy, in *Phase Transitions and Critical Phenomena*, Vol. 11, edited by C. Domb and J. L. Lebowitz (Academic, New York, 1987).
[14] H. W. J. Blöte, J. L. Cardy, and M. P. Nightingale, Phys. Rev. Lett. **56**, 742 (1986); I. Affleck, *ibid.* **56**, 746 (1986).
[15] J. A. Plascak, J. G. Moreira, and F. C. Sá Barreto, Phys. Lett. A **173**, 360 (1993).
[16] M. N. Tamashiro and S. R. A. Salinas, Physica A **172**, 378 (1991).
[17] P. M. C. de Oliveira, Europhys. Lett. **20**, 621 (1992).
[18] A. Bakchich, A. Bassir, and A. Benyoussef, Physica A **195**, 188 (1993).
[19] E. Fradkin and L. Susskind, Phys. Rev. D **17**, 2637 (1978); J. B. Kogut, Rev. Mod. Phys. **51**, 659 (1979).
[20] A. Jennings and J. J. Mckeown, *Matrix Computation* (Wiley, New York, 1983), p. 233.
[21] M. N. Barber, in *Phase Transitions and Critical Phenomena*, Vol. 8, edited by C. Domb and J. L. Lebowitz (Academic, New York, 1983), p. 145.
[22] M. E. Fisher and N. Berker, Phys. Rev. **26**, 2707 (1982); P. A. Rikvold, W. Kinzel, J. D. Gunton, and K. Kaski, Phys. Rev. B **28**, 2686 (1983); H. J. Hermann, Phys. Lett. A **100**, 156 (1984).
[23] A. L. Malvezzi, Braz. J. Phys. **24**, 508 (1994); K. Becker, M. Becker, and G. von Gehlen (unpublished).
[24] J. M. van den Broeck and L. W. Schwartz, SIAM (Soc. Ind. Appl. Math.) J. Math. Anal. **10**, 658 (1979); C. J. Hamer and M. N. Barber, J. Phys. A **14**, 2009 (1981).
[25] D. Sen, Phys. Rev. B **44**, 2645 (1991).
[26] K. Binder, *Monte Carlo Methods in Statistical Physics* (Springer-Verlag, Berlin, 1979), Chap. 1.